

# Cavity Ring-Down Polarimetry (CRDP): A New Scheme for Probing Circular Birefringence and Circular Dichroism in the Gas Phase

Thomas Müller, Kenneth B. Wiberg, and Patrick H. Vaccaro\*

Department of Chemistry, Yale University, New Haven, Connecticut 06520-8107

Received: February 22, 2000; In Final Form: April 17, 2000

Cavity ring-down polarimetry (CRDP), a new, ultrasensitive method for probing circular birefringence and circular dichroism, has been developed by extending the well-established technique of pulsed cavity ring-down spectroscopy (CRDS). The concurrent incorporation of polarization elements into the stable resonator, injection optics, and detection train of a conventional CRDS apparatus is found to permit the quantitative measurement of optical rotation and differential absorption induced by the presence of chiral compounds. The sensitivity of this novel scheme is sufficient to allow (low-pressure) gas-phase species to be interrogated under ambient conditions, a fact highlighted by the direct determination of specific rotation at 355 nm ( $[\alpha]_{355\text{nm}}^{25^\circ\text{C}}$ ) for gaseous samples of  $\alpha$ -pinene,  $\beta$ -pinene, *cis*-pinane, limonene, fenchone, and propylene oxide. Although usually precluded by the signal discrimination limits imposed upon traditional polarimeters, such gas-phase studies of nonresonant optical activity in the visible and near-ultraviolet regions of the electromagnetic spectrum can serve to calibrate ab initio theoretical predictions and to examine the roles of solvent–solute interactions. Comparison of the CRDP-measured specific rotation angles for isolated (gaseous) chiral molecules with analogous solution-phase results reveals that solvent effects can be significant and nonintuitive, often leading to solvent-mediated  $[\alpha]_{355\text{nm}}^{25^\circ\text{C}}$  values that differ significantly from their gas-phase counterparts in both magnitude and sign.

## I. Introduction

The chiral nature of molecules and their interactions play pivotal roles in a wide variety of chemical<sup>1</sup> and biological<sup>2</sup> processes. The circular birefringence and circular dichroism (CD) exhibited by pure substances possessing this unique property of intrinsic “handedness” afford a robust, nonintrusive, and quantitative means for species discrimination.<sup>3</sup> It long has been recognized that the two molecules comprising an enantiomeric pair lead to optical rotatory dispersion (ORD) and CD spectra that are the exact opposite of one another;<sup>4,5</sup> however, the precise correlation of an individual enantiomer with a given optical behavior still requires the use of supplementary physical and/or chemical information. Indeed, despite a history of polarization rotation and differential absorption measurements that extends back nearly to the beginning of the 19th century,<sup>6,7</sup> it did not prove feasible to identify the absolute configuration of an enantiomer until 1951, when Bijvoet and Peerdeman<sup>8</sup> exploited X-ray crystallography to unambiguously assign sodium rubidium tartrate. While our ability to unravel and interpret molecular phenomena has been augmented greatly by the advent of computationally expedient quantum chemistry,<sup>9</sup> the theoretical prediction of optical activity and accompanying determination of absolute configuration remains a formidable challenge.<sup>10,11</sup> The inherent difficulty of this task is compounded by the fact that the vast majority of laboratory data available for comparison with theory stems from experiments conducted in the solution phase. Consequently, ab initio analyses need to account both for the optical response evoked from an isolated molecule and for the perturbations incurred by presence of the solvent medium. Although Biot reported the qualitative rotation of

optical polarization in vapors produced by boiling turpentine as early as 1817,<sup>6</sup> the stringent demands placed upon detection limits has precluded all but a handful of semiquantitative gas-phase polarimetric studies.<sup>7,12</sup> The present work strives to remedy this situation by providing detailed measurements of nonresonant optical activity for isolated (gas-phase) chiral species maintained under ambient (room-temperature) conditions. Cavity ring-down polarimetry (CRDP), a novel technique for probing circular birefringence and circular dichroism with unprecedented sensitivity, has been developed and implemented for this purpose. Direct comparison of our gas-phase specific rotation values with analogous solution-phase results highlights the pronounced and complex effects induced by solvation.

The influence of solvent–solute interactions upon optical activity has been the subject of numerous experiments, including extensive studies examining chiral solutes dissolved in achiral media<sup>13–15</sup> as well as more limited efforts exploring the induction of circular dichroism in achiral molecules by the presence of chiral solvents<sup>16</sup> or contact ion pairs.<sup>17</sup> While comparison of ORD data sets recorded in diverse liquids can provide an estimate for the magnitude of solvent effects,<sup>15,18</sup> additional insight often can be gleaned from solvent-induced perturbations in transition energies, vibronic intensities, and differential absorption properties.<sup>15</sup> It long has been known that ORD curves display complicated patterns in the vicinity of an electronic absorption band (the Cotton effect),<sup>5</sup> with the use of different solvents leading to both spectral shifts and intensity alterations.<sup>15</sup> Obviously, the quantitative elucidation of solvation phenomena and the critical assessment of ab initio predictions for optical response could benefit greatly from measurements performed on isolated (gas-phase) species. Since circular birefringence (i.e., responsible for nonresonant polarization

\* To whom correspondence should be addressed. E-mail: patrick.vaccaro@yale.edu. Telephone/Fax Number: (203) 432-3975/(203) 432-6144.

rotation) and circular dichroism (i.e., responsible for resonant differential absorption) are interconnected by a Kronig–Kramers relationship (viz., akin to that existing between the linear index of refraction and linear absorption coefficient),<sup>19</sup> the unique ORD and CD behavior of a target molecule can be calculated (in theory) from one another, provided that highly refined information is available over a sufficient range of excitation frequencies. The complementary techniques of vibrational circular dichroism<sup>20,21</sup> (VCD) and Raman optical activity<sup>21,22</sup> (ROA), which probe the weak CD patterns ascribed to fundamental vibrational bands, have been employed primarily for target molecules entrained in liquid media; however, a limited number of gas-phase VCD investigations have been reported<sup>23</sup> for compounds possessing sufficient volatility. Although purported to exhibit less pronounced perturbations from the presence of solvent than is the case for analogous ultraviolet/visible measurements,<sup>24</sup> these experimental efforts, in conjunction with supporting theoretical analyses,<sup>25</sup> have documented the important role played by solvent-induced conformational changes in the appearance of VCD and ROA spectral features. A variety of gas-phase CD results have been interpreted in the vacuum-ultraviolet (VUV) region,<sup>26,27</sup> where the total and differential absorption cross sections are significantly larger than those encountered at longer wavelengths. Such VUV work can furnish substantial and otherwise unobtainable insight regarding the nature of electronically excited states; however, it neither lends itself readily to the interrogation of solvent effects nor enables potentially successful *ab initio* calculations to be extrapolated directly into the chemically relevant near-ultraviolet/visible portion of the spectrum.

Poirson and co-workers<sup>28</sup> recently demonstrated a high-sensitivity polarimeter that permits the detection of circular birefringence and circular dichroism under rarefied conditions. This pioneering work exploited a Fabry–Perot resonator, which was servo-locked to a frequency-stabilized helium–neon laser source, with the chiral target molecules entrained between two intracavity quarter waveplates. In comparison to a conventional single-pass instrument, this cavity-enhanced polarimetry (CEP) configuration afforded a signal enhancement factor of  $4KF^2/\pi^2$ , where  $K$  and  $F$  denote the Fabry–Perot transmission coefficient and finesse, respectively. While Poirson et al. did show the ability to observe gas-phase optical activity, they did not report quantitative measurements, owing, presumably, to limitations inherent in the design of their apparatus (e.g., the vacuum integrity of their sample vessel was compromised by employing the thin intracavity  $\lambda/4$ -retarders as windows). The experimental efforts discussed below build, in part, upon the technical innovations introduced by these authors; however, since the rotation rate is monitored rather than the cumulative rotation angle, our method dispenses with the need for sophisticated frequency/cavity stabilization schemes (e.g., laser frequency stabilization combined with active cavity-length modulation) and enables the facile extraction of quantitative information regarding circular birefringence as well as circular dichroism.

The aforementioned measurement of rotation rates for the polarization vector of an interacting electromagnetic field rather than the corresponding cumulative rotation angle is analogous to the distinction that exists between traditional absorption spectroscopy and the burgeoning technique of cavity ring-down spectroscopy (CRDS).<sup>29</sup> More specifically, CRDS dispenses with the need to monitor the overall attenuation of an impinging optical wave and instead focuses on the observation of accompanying attenuation rates. In its canonical form, a short burst of tunable laser radiation is injected into an optically stable,

high-finesse cavity containing the target medium and the absolute absorbance of the sample follows directly from the time constant imposed upon the exponentially decaying train of outcoupled light pulses. This approach yields long effective path lengths (i.e., corresponding to anywhere from hundreds to thousands of round-trip passes through the cavity) and essentially is immune to noise problems arising from intensity fluctuations in the excitation source. While a continuous-wave (monochromatic) ring-down reflectometer had been demonstrated by Anderson and co-workers as early as 1984,<sup>30</sup> it was not until the subsequent development of the pulsed ring-down methodology by O’Keefe and Deacon<sup>31</sup> that this ultrasensitive absorption probe has come into widespread use. Many variations of the basic CRDS scheme have been documented,<sup>32,33</sup> including an implementation of polarization spectroscopy by Engeln et al.,<sup>34</sup> which was designed to investigate magneto-optical rotation in gases and transparent solids as well as magnetic circular dichroism in gaseous media. These authors measured magnetically induced polarization rotation rates as low as  $10^{-8}$  rad/cm and achieved an ultimate differential absorption detection limit of  $\sim 3 \times 10^{-9}$  cm<sup>-1</sup>, thereby demonstrating sufficient gas-phase sensitivity to interrogate not only optical rotation generated through application of external magnetic fields but also, in theory, that arising from intrinsic molecular chirality.

The seminal work of Engeln et al.,<sup>34</sup> has demonstrated sufficient sensitivity for the measurement of nonresonant gas-phase optical activity by means of CRDS; however, straightforward application of this approach to the investigation of “field-free” or “natural” optical activity is hampered by the fundamental differences that distinguish magnetically-induced polarization effects from their chirality-induced counterparts. In particular, the physical observables corresponding to optical rotation can be classified according to their behavior under transformations specified by the space-inversion (or parity),  $\hat{\Pi}$ , and time-reversal,  $\hat{\Theta}$ , operators. For this analysis only the target sample and any applied external fields, rather than the entire experiment (i.e., including the polarized light source), need be considered; otherwise, one would merely confirm the expected conservation of parity and temporal reversibility (i.e., so long as the influence of weak nuclear forces is excluded).<sup>35</sup> While the magneto-optical effect can be shown to have even and odd symmetries under the action of  $\hat{\Pi}$  and  $\hat{\Theta}$ , respectively, natural chirality exhibits the opposite spatial and temporal characteristics, being odd in parity (parity-odd) and even in time (time-even).<sup>36</sup> As discussed below, this disparity in symmetry properties profoundly influences the manifestation of polarization rotation phenomena in an optical cavity.

Since the transformation generated by  $\hat{\Theta}$  will reverse the relative orientation of an applied magnetic field with respect to the propagation direction of an interacting light beam, the sign of polarization rotation in a magneto-optical process will be switched upon reflection from the end mirrors of a CRDS apparatus. Consequently, optical radiation which traverses the target medium, impinges upon a mirror surface, and emerges back through the same molecular sample will accrue a net polarization rotation (i.e., the polarization vector of the reflected wave experiences a rotation of opposite sense with respect to the new direction of propagation). In contrast, the fact that “natural” optical rotation does not change sign under the influence of time reversal symmetry will lead to an overall cancellation of polarization effects during each round-trip pass through a linear resonator cavity, thereby precluding straightforward application of the CRDS methodology for the investigation of optical activity in chiral molecules.

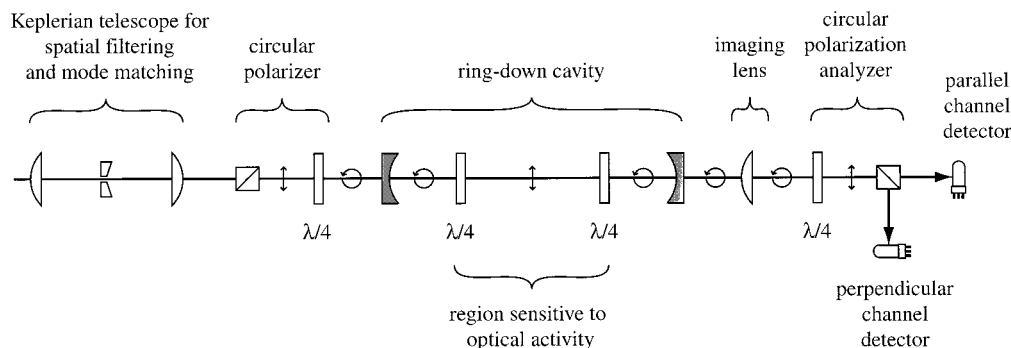


**Figure 1.** Schematic diagram of cavity ring-down polarimetry (CRDP) apparatus. Pulsed ultraviolet radiation at 355 nm is spatially filtered and mode-matched for the CRDP resonator before traversing a circular polarizer consisting of a tandem calcite prism (linear polarizer) and quarter waveplate. The resulting beam is coupled into a stable linear cavity of 1.63 m length by passing through the planar rear surface of the input mirror (NB: both mirrors have a nominal 1 m radius of curvature). Intracavity  $\lambda/4$ -retarders, located 17 cm from each mirror, are aligned to produce a linearly polarized internal field over the intervening 1.29 m region, thereby making this portion of the ring-down apparatus sensitive to the effects of optical activity. Light emerging from the output mirror is imaged onto identical photodetectors that monitor two mutually orthogonal components of linear polarization generated by means of a circular polarization analyzer.

For the effects of chirality to accumulate in a stable linear resonator despite their intrinsic time-even symmetry, the sign of the optical rotation acquired during a single pass must be reversed upon reflection. As demonstrated by the Fabry–Perot work of Poirson et al.,<sup>28</sup> this task can be accomplished readily by preceding each cavity mirror with a quarter waveplate. When linearly-polarized radiation traverses a  $\lambda/4$ -retarder, impinges upon a highly reflective surface, and emerges back through the same phase retarder, the electric field vector,  $\mathbf{E}$ , will be inverted through a plane containing the propagation wave vector,  $\mathbf{k}$ , and the fast axis of the waveplate,  $\mathbf{n}_f$ . Consequently, the sign of the angle (i.e., the sense of accrued optical rotation) between  $\mathbf{E}$  and  $\mathbf{n}_f$  is switched when viewed along the original direction specified by  $\mathbf{k}$ . To maintain a fixed linear polarization state in an evacuated multipass cavity (viz., sans chiral medium), the internal  $\lambda/4$ -retarders must have their fast axes aligned to be either mutually parallel or, alternatively, at right angles to one another. Obviously, successful integration of this approach with the pulsed CRDS methodology, as required for the present implementation of cavity ring-down polarimetry, will demand that the surfaces of all intracavity components be treated with antireflection coatings of exceptional efficiency.

## II. Experimental Methods and Alignment Procedures

For the present studies, the requisite 355 nm radiation was generated by frequency doubling the fundamental output of a moderate-resolution dye laser (Lambda Physik FL3002E;  $<0.15$   $\text{cm}^{-1}$  bandwidth) which was pumped by the second harmonic of an injection-seeded Nd:YAG system (Spectra Physics GCR-4-20; 20 pps). The resulting ultraviolet light was isolated by a set of Brewster angle prisms and propagated through a variable attenuator before entering a Keplerian telescope, where it was spatially filtered and focused to match the  $\text{TEM}_{00}$  cavity mode of the ring-down apparatus. As illustrated by the schematic experimental diagram in Figure 1, a calcite prism (linear polarizer) and multiple-order quarter ( $\lambda/4$ ) waveplate were used in tandem to produce an input beam of well-defined circular polarization.

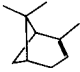
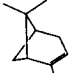
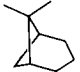
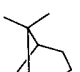
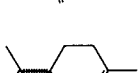
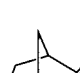
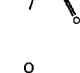
The ring-down cavity was constructed from an identical pair of concave mirrors (Research Electro-optics, Inc.), characterized by a 1 m radius of curvature and a reflectivity of  $>99.95\%$  centered at 355 nm, which were O-ring-sealed to adjustable (tiltable/translatable) mounts and separated by a path length of 1.63 m. Two multiple-order quarter waveplates (VLOC, Inc.; retardation tolerance  $\lambda/200$ – $\lambda/600$ , transmitted wave front  $\lambda/10$

at 632.8 nm) having efficient 355 nm antireflection coatings that gave rise to a total loss of  $\sim 0.18\%$  per surface were placed into the optical resonator at a distance of 17 cm from each end mirror, thereby making the polarization state of radiation in the intervening 1.29 m region sensitive to the circular birefringence and circular dichroism of an entrained (chiral) sample. The entire apparatus was evacuated by means of a liquid-nitrogen-baffled oil diffusion pump, resulting in a base pressure for the empty cavity of  $<10^{-6}$  Torr as measured by an uncalibrated ionization gauge.

The polarization state of the optical field propagating between the intracavity waveplates was analyzed by projecting it onto two orthogonal linear axes, a task accomplished by incorporating a quarter waveplate and calcite prism into the detection train. Each (linearly polarized) signal component was measured by means of a separate photomultiplier tube (Hamamatsu 1P28A), with the resulting pair of ring-down traces being displayed upon a digitizing oscilloscope (Tektronix TDS684B) which permitted signal averaging (typically over 4000 laser shots) as well as transfer of acquired data to a personal computer for further processing. Since the temporal duration of the impinging laser pulses ( $\sim 7$  ns) was slightly shorter than the round-trip time in the stable optical cavity ( $\sim 11$  ns), partially resolved mode-related structure was found to be superimposed upon the exponentially decaying (ring-down) profile. Reduction of the oscilloscope bandwidth from its full 1 GHz value to a nominal 25 MHz figure through use of an internal electronic filter provided an effective means for discriminating against these undesirable features.

The (1*R*,5*R*)-(+)- $\alpha$ -Pinene, (1*S*,5*S*)-(–)- $\alpha$ -pinene, (1*S*,5*S*)-(–)- $\beta$ -pinene, (1*R*)-(+)-limonene, (1*R*)-(–)-fenchone, and the (1*S*)-(–)-propylene oxide examined in the present study were acquired from a commercial source (Aldrich Chemical Co.), while (1*S*)-(–)-*cis*-pinane was obtained from the catalytic reduction<sup>37</sup> of (1*S*)-(–)- $\alpha$ -pinene. Table 1 contains a compilation of the chemical and enantiomeric purities estimated for the liquid phase of these chiral compounds. To prevent disproportionate contamination of the vapor phase, each compound was subjected to at least three freeze–pump–thaw cycles prior to use. Sample pressures were set between 0.5 and 10 Torr, as measured by factory-calibrated capacitance manometers (MKS Baratron 627 and 722), and typically changed by  $<5$  mTorr during the acquisition of ring-down traces. The CRDP values of gas-phase specific rotation at 355 nm were compared with analogous solution-phase quantities, the latter being extrapolated from

TABLE 1: Results of Specific Rotation Measurements<sup>a</sup>

| Optically active sample   | Purity       | Specific rotation [ $\alpha$ ] <sub>355nm</sub> <sup>25°C</sup> |                               |
|---|--------------|---|-------------------------------|
|   |              | gas-phase (measured)  | solution-phase (extrapolated) |
| (1 <i>R</i> ,5 <i>R</i> )-(+) - $\alpha$ - Pinene  | ≥99% (97%ee) | 191.2 ± 2.8   | 165.2                         |
| (1 <i>S</i> ,5 <i>S</i> )-(-) - $\alpha$ - Pinene  | 99% (97%ee)  | -188.8 ± 2.8  | -165.2                        |
| (1 <i>S</i> )-(-) - <i>cis</i> - Pinane            | 99%          | -63.0 ± 5.9   | -88.4                         |
| (1 <i>S</i> ,5 <i>S</i> )-(-) - $\beta$ - Pinene   | ≥99% (97%ee) | 70.5 ± 2.0  | 21.8                          |
| ( <i>R</i> )-(+)-Limonene                          | 97% (98%ee)  | 304.2 ± 11.0  | 416.9                         |
| (1 <i>R</i> )-(-)-Fenchone                         | ≥98%         | -180.3 ± 9.3  | -157.8                        |
| ( <i>S</i> )-(-)-Propylene oxide                  | 99%          | 10.2 ± 2.9  | -26.4                         |

<sup>a</sup> For each of the chiral species examined in this study, the specific 355 nm optical rotation determined under ambient laboratory conditions, [ $\alpha$ ]<sub>355nm</sub><sup>25°C</sup>, is tabulated in the canonical units of deg dm<sup>-1</sup> (g/mL)<sup>-1</sup>. Values obtained for isolated gas-phase samples (i.e., as measured from cavity ring-down polarimetry) and cyclohexane solution-phase samples (i.e., as extrapolated from conventional rotatory dispersion data) are presented. The chemical and enantiomeric purities of the target compounds also are listed, with the latter being specified as the enantiomeric excess revealed by gas-liquid chromatography. Disproportionate vapor-phase contamination was avoided by subjecting liquid molecular samples to several freeze-pump-thaw cycles prior to use.

rotatory dispersion data acquired at five distinct wavelengths (viz., 589, 578, 546, 436, and 365 nm) through use of a commercial polarimeter (Perkin-Elmer 341) equipped with sodium and mercury atomic emission lamps. Cyclohexane and acetone solvents of spectral quality were employed, with sample concentrations adjusted to yield reasonable optical rotation angles for the experimental path length of 1 dm.

Successful implementation of the CRDP scheme required proper alignment of the polarization elements depicted in Figure 1 by means of the following multiple-step procedure. The cavity mirrors and all waveplates (viz., the two intracavity  $\lambda/4$ -retarders as well as those placed in the incident beam and detection train) first were removed, leaving behind two calcite prism polarizers located, respectively, in the input (before cavity) and output (after cavity) beams, the latter of which was then rotated in order to extinguish the transmitted portion of the impinging linearly polarized 355 nm radiation. The first quarter waveplate (i.e., situated in the input beam) was installed and adjusted to produce circularly polarized light by nulling the intensity of a retroreflection that counterpropagated through this  $\lambda/4$ -retarder as well as the preceding calcite prism. The fast axis of the second quarter waveplate was brought into coincidence with the slow axis of the first  $\lambda/4$ -retarder by canceling the output emerging from the final calcite prism. In a similar manner, alignment of the third quarter waveplate was facilitated by employing a back-

reflection through all three  $\lambda/4$ -retarders and the input calcite polarizer. Finally, the fourth quarter waveplate was positioned by zeroing the transmitted light from the entire assembly of four  $\lambda/4$ -retarders and two calcite prisms. Following reinsertion of the resonator mirrors as well as a plano-convex lens designed to image the signal beam onto the detectors, the intracavity waveplates were fine-tuned by monitoring the pair of polarization-resolved ring-down signals displayed on the digitizing oscilloscope. Initial traces typically showed oscillations (i.e., arising from the changing polarization state of the internal field during successive round trips through the optical cavity) which could be eliminated by precise alignment of the intracavity retarders. This task required mounting of the (intracavity) waveplates in custom-built stages that enabled them to be rotated in vacuo about two mutually orthogonal axes, one of which coincided with the direction of beam propagation.<sup>38</sup>

The incorporation of a calcite polarizer into the detection train permitted two mutually orthogonal (linearly-polarized) projections of the signal wave to be isolated and monitored on separate channels of the digitizing oscilloscope. With the transmission axis of this linear polarization element set orthogonal to that of the calcite prism in the input beam, final alignment of the intracavity waveplates was complete when the "parallel" channel (i.e., signal component parallel to input polarization) displayed an unmodulated ring-down profile while the corresponding



“perpendicular” channel (i.e., signal component orthogonal to input polarization) showed no response. Under ideal circumstances, this arrangement furnishes a pair of time-resolved data sets that directly reflect the polarization state of the optical field propagating between the internal  $\lambda/4$ -retarders (N.B.: this field will remain linearly polarized in the presence of circular birefringence but will evolve slowly to a state of circular polarization if circular dichroism exists). Admission of a chiral gas-phase sample to the resonator assembly reestablishes a nonzero rate of polarization rotation, thereby leading to a slow modulation of the exponentially decaying “parallel” trace and the concomitant appearance of a (slowly modulated) signal in the previously nulled “perpendicular” channel. The portion of the 355 nm excitation pulse emerging from the cavity output mirror during each round-trip pass thus provides a means of accurately measuring the polarization rotation frequency,  $\omega$  (in units of rad/s or, equivalently, rad/pass), over long effective path lengths, with the optical activity of an entrained (chiral) medium responsible for introducing a change in rotation frequency,  $\Delta\omega$ . There are many possible ways to envision the substantial array of optical components comprising the cavity ring-down polarimeter, one of the most fruitful of which considers all elements to be grouped into a pair of identical sets, each consisting of the calcite prism and two waveplates located on opposite sides of the apparatus. When properly aligned, these elements are designed to function as linear-polarization “projectors” which allow a round-trip-stable electromagnetic wave of linear polarization to be injected into the region of chiral sensitivity for the empty cavity (i.e., the volume encompassed by the intracavity retarders) and enable any modifications introduced into this internal field by an optically active target medium to be examined quantitatively through subsequent decomposition into linear components.

In principle, the CRDP scheme allows for the background-free determination of gas-phase optical activity by setting the polarization rotation frequency of the empty apparatus equal to zero,  $\omega_0 = 0$ , and monitoring the change,  $\Delta\omega$ , induced by the presence of a chiral compound maintained at a known total pressure. However, the practical implementation of this approach was hampered by the finite polarization contrast ratio exhibited by 355 nm radiation emerging from the ring-down cavity which, in the absence of sophisticated compensation elements, could not be described as a pure state of circular polarization and, therefore, was not transformed into pure linear polarization upon subsequent propagation through the  $\lambda/4$ -retarder incorporated into the detection train. As a result, a small residual background remained in the nominally nulled “perpendicular” channel and the ability to extract quantitative optical activity information from such  $\omega_0 = 0$  studies was compromised. A further complication was found in the limited mechanical and thermal stability of the present ring-down oscillator, which was based upon a versatile vacuum chamber that had been designed primarily for molecular beam studies of linear and nonlinear spectroscopy.<sup>39</sup> Without the benefits of active stabilization, the optical path length of light travelling through the intracavity multiple-order waveplates varied slightly over the course of minutes to hours. Amplified by hundreds of passes through the cavity, where each round trip was accompanied by four traversals of internal waveplates, the resulting variations in phase retardation produced significant alternations in polarization state that, once again, hindered the ability to perform meaningful optical activity measurements in a zero-background configuration.

The present experiments employed a modified detection method that retains the advantages of high sensitivity while

alleviating the demands imposed upon mechanical/thermal stability and polarization contrast ratio. After the alignment procedure outlined above was performed, the intracavity waveplate nearest to the output mirror was rotated by a few degrees so as to produce an internal field that remained linearly polarized with its direction of polarization changing during each successive traversal of the empty resonator (i.e.,  $\omega_0 \gg 0$ ). Under such conditions, both signal channels displayed rapid oscillations superimposed upon exponentially decaying profiles, with the period of modulation selected to be much shorter than the ring-down time but substantially longer than the duration of a single round trip through the cavity. As found for the stationary ( $\omega_0 = 0$ ) configuration, the difference in rotation frequency between the empty and filled apparatus,  $\Delta\omega$ , provides a quantitative measure for gas-phase optical activity. The modulation approach offers several crucial advantages over the aforementioned zero-background technique. The observation of many full oscillation periods furnishes a simple means for extracting  $\omega$  (vide infra), which is nearly independent of polarization purity so long as a finite excess of linear polarization continues to propagate in the region between the internal  $\lambda/4$ -retarders. A marked reduction in the influence of resonator instabilities follows from the observation that the tilt angles ( $\phi$ ) for the intracavity waveplates, rather than their rotation angles ( $\theta$ ) about the beam propagation direction, were most susceptible to the effects of mechanical and thermal noise. Fluctuations in  $\theta$  would affect the relative orientation of fast axes, thereby changing the amplitudes of retarded linear components and, after successive round trips, introducing substantial errors into the polarization state (i.e., direction of linear polarization) of the entrained electromagnetic field. In contrast, the noted sensitivity of  $\phi$  influences only the retardation path length (i.e., retardation phase) and leads to a moderate increase in polarization ellipticity. Simulations of this phenomenon through Jones Matrix Calculus<sup>40</sup> demonstrated that  $\omega$  values deduced from the modulation technique will remain essentially unchanged even in the presence of significant retardation imperfections (e.g., the modulation scheme is predicted to yield accurate measurements of  $\omega$  even for imperfections sufficient to produce a 50% loss in modulation depth at the end of the ring-down trace).

While the experimental work discussed below has focused on gas-phase circular birefringence, analogous circular dichroism information can be obtained in a straightforward manner. In particular, differential absorption of circular components will manifest itself as the gradual conversion of linear polarization to circular polarization in the region surrounded by the intracavity waveplates, thereby leading to a progressive loss of modulation depth in the oscillating ring-down traces (cf. the preceding paragraph). An analysis of the damping rate affecting these polarization oscillations should permit the quantitative extraction of circular dichroism data. An alternative and more direct measurement could be performed by removal of the  $\lambda/4$ -retarder in the detection train, enabling the quarter waveplate in proximity to the output mirror and the following calcite prism to function (in combination) as a circular polarization analyzer. In this case, the change in ring-down lifetime between the pair of signal channels (i.e., still monitoring orthogonal projections of linear polarization) would reflect the differential attenuation of the two circular polarization components in the cavity.

### III. Results and Discussion

Figure 2 presents typical CRDP results obtained consecutively for an evacuated apparatus (solid line) and one containing a 1.43 Torr sample of (1*S*,5*S*)-(–)- $\alpha$ -pinene (dashed line). Each

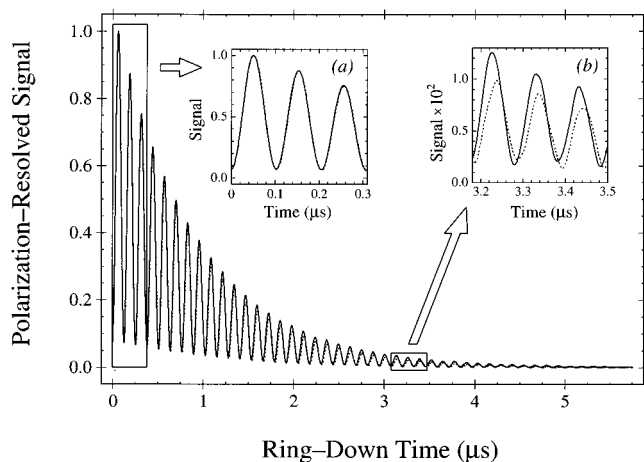


**Figure 2.** Temporal traces acquired through use of cavity ring-down polarimetry (CRDP). The relative intensity of light transmitted through a cavity-enhanced polarimeter is plotted as a function of time,  $t$ , where the reference value of  $t = 0$  corresponds to the instant that the 355 nm excitation pulse first enters the apparatus (see text for further details). The polarization-resolved ring-down traces are comprised of 5000 discrete points and are displayed both for an empty cavity ( $\ll 1$  Torr; solid line) and for one containing  $\sim 1.5$  Torr of room-temperature (1*S*,5*S*)-(-)- $\alpha$ -pinene (dashed line). The insets provide expanded views of the response measured in the vicinity of (a)  $t = 0$  and (b)  $t = 3.2$   $\mu$ s, where the latter data have been subjected to a 50-pass Gaussian (binomial) smoothing in order to reduce high-frequency noise. Comparison of the two curves in this figure highlights the shift in (polarization) oscillation frequency caused by presence of the gas-phase chiral sample.

trace represents the digitized and averaged response generated by 4000 individual laser pulses, with the selected 355 nm wavelength of the excitation source being far removed from known absorption features of the target species.<sup>27</sup> While the finite reflectivity of the cavity mirrors produced photon lifetimes in excess of 5  $\mu$ s, the insertion of intracavity waveplates for polarimetric measurements introduced significant losses that reduced ring-down times to  $\sim 700$  ns. The depicted polarization-resolved data were acquired in the “perpendicular” signal channel (i.e., signal component orthogonal to linear input polarization) and the analogous “parallel” channel, which was recorded concurrently, gave similar curves having modulations shifted by an overall phase factor of  $\pi$ . The insets of Figure 2 provide enlarged views of the exponentially decaying profiles over two distinct time intervals, highlighting the fact that polarization oscillations still are discernible after elapsed times of  $\geq 3$   $\mu$ s, which correspond to effective sample path lengths longer than 1 km. More importantly, the signal modulations observed in the presence of the chiral (1*S*,5*S*)-(-)- $\alpha$ -pinene molecules are found to be displaced visibly from those of the empty apparatus, an effect that becomes progressively more pronounced as the decay time (or, equivalently, the sample interaction path length) increases (cf., insets (a) and (b) of Figure 2). Inset (b) reveals a slight loss in ring-down amplitude to take place when the 355 nm radiation traverses the low-pressure gaseous medium. This phenomenon can most directly be attributed to resonant absorption processes; however, the nearest electronically allowed transition of  $\alpha$ -pinene resides in the vacuum-ultraviolet region<sup>27</sup> with no appreciable absorption reported above 200–220 nm.

Fourier transformation of the ring-down traces depicted in Figure 2 reveals the dominant frequency component to be that of the polarization rotation,  $\omega$ , with small secondary contributions arising from the cavity round-trip frequency as well as their sums and differences. While the value of  $\omega$  can be extracted

from such Fourier analyses, the present work made use of a robust time-domain treatment based upon nonlinear least-squares regression of the observed CRDP signal intensity,  $I(t)$ , to a model functional form. For an exponentially decaying envelope characterized by effective lifetime  $\tau$ , an appropriately parameterized expression for  $I(t)$  was found to be given by

$$I(t) = Ae^{-t/\tau}[\sin^2(\omega t + \varphi) + B] \quad (1)$$

where  $A$  scales the overall signal amplitude,  $\varphi$  represents a global phase offset, and parameter  $B$  takes into account the reduction in modulation depth stemming from nonzero polarization ellipticity. As discussed in section II, the rate of optical rotation induced by the gas-phase chiral species follows directly from the difference,  $\Delta\omega$ , between  $\omega$  values determined for the filled and empty chambers. Since the CRDP apparatus is sensitive only to circular birefringence/dichroism in the region encompassed by the two intracavity waveplates,  $\Delta\omega$  must be corrected for the reticent fraction of the polarimeter that exists between the cavity mirrors and the internal  $\lambda/4$ -retarders. Once this adjustment has been made and the uniform number density of the target molecules has been ascertained from the measured sample pressure, it is straightforward to calculate the corresponding 355 nm specific rotation in the canonical units of  $\text{deg dm}^{-1} (\text{g/mL})^{-1}$ ,  $[\alpha]_{355\text{nm}}^{25^\circ\text{C}}$ , where the superscript 25  $^\circ\text{C}$  indicates that this quantity has been obtained at room temperature.

Table 1 contains a compilation of  $[\alpha]_{355\text{nm}}^{25^\circ\text{C}}$  values determined under ambient gas-phase conditions for each of the chiral species examined during this investigation. The tabulated 1 standard deviation confidence limits, derived through propagation of the errors ascribed to extracted modulation frequencies and measured sample pressures, are in good accord with the reproducibility achieved by repeating experiments on multiple days. Before attributing these specific rotations to pure substances, it is useful to consider the possible effects incurred by chemical/enantiomeric impurities. On one hand, only a portion of the liquid-phase material was in enantiomeric excess (cf., Table 1 for enantiomeric purity) and was capable of contributing to the observed optical activity, with the remaining fraction presumed to be an optically inactive racemic mixture. Furthermore, other optically active contaminants (cf., Table 1 for chemical purity) could modify the observed CRDP response by an unknown amount. While neither of these issues can be eliminated a priori, analogous solution-phase studies (vide infra) suggest their influence to be of minor importance. The overall reliability of the CRDP technique was assessed by performing analyses on the achiral vapor of cyclohexane, leading to the expected null result for  $[\alpha]_{355\text{nm}}^{25^\circ\text{C}}$ . Likewise, the pair of  $\alpha$ -pinene enantiomers was found to have gas-phase specific rotation values of equal magnitude yet opposite sign, at least to within the precision imposed by measurement uncertainty and enantiomeric/chemical purity (cf., Table 1). Finally, the scaling of CRDP response with sample pressure was probed for  $\alpha$ -pinene over the 0.4–2.0 Torr range, yielding the predicted linear dependence of  $[\alpha]_{355\text{nm}}^{25^\circ\text{C}}$  on target number density.

To elucidate the influence of solvent–solute interactions upon optical activity, solution-phase measurements were performed on each of the targeted chiral compounds through use of a commercial polarimeter. The good agreement between these (solution-phase) results and those reported previously in the published literature served to validate the chemical and enantiomeric purity of our molecular samples. Figure 3 presents a comparison of optical rotatory dispersion (ORD) spectra obtained for (1*S*,5*S*)-(-)- $\alpha$ -pinene in both acetone and cyclohexane

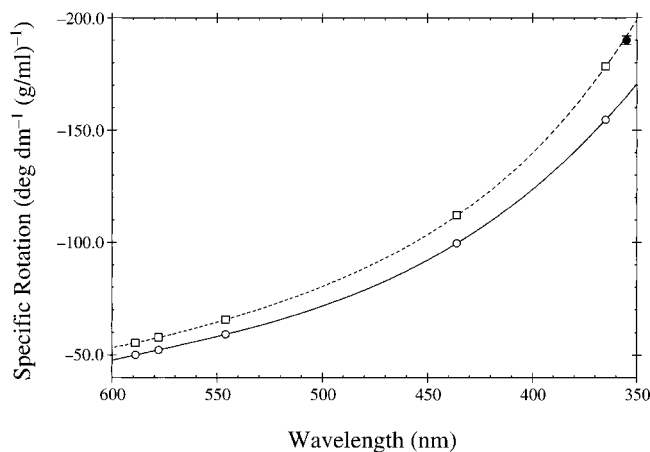


**Figure 3.** Gas-phase optical rotation of (1*S*,5*S*)-(-)- $\alpha$ -pinene compared with its solution-phase rotatory dispersion spectrum. The specific rotation of (1*S*,5*S*)-(-)- $\alpha$ -pinene in units of  $\text{deg dm}^{-1} (\text{g/mL})^{-1}$  is plotted as a function of wavelength. Solution-phase rotatory dispersion data were obtained at five discrete wavelengths for both cyclohexane (open circles connected by solid line) and acetone (open squares connected by dashed line) solutions of roughly 100 mg/L concentration. The filled circular symbol at 355 nm denotes the CDRP-measured gas-phase value with the accompanying error bars representing a 1 standard deviation uncertainty limit.

solutions, with the CDRP-measured (gas-phase) specific rotation displayed as a single data point at 355 nm. Given the similar shapes of these curves, the absence of hydrogen bonds or conformation changes involving the solute, and the relative polarity of the selected solvent media, simple models of solvent-solute interactions, such as those based upon reaction field theory,<sup>41</sup> would predict larger solvent effects to be operational in the case of acetone.<sup>14,15</sup> In contrast, inspection of the information available at 355 nm (cf. Figure 3 and Table 1) shows the acetone-mediated value of  $[\alpha]_{355\text{nm}}^{25^\circ\text{C}}$  for (1*S*,5*S*)-(-)- $\alpha$ -pinene to reproduce that determined for the isolated (gas-phase) molecule to within 1%, while the corresponding cyclohexane result is roughly 15% lower in magnitude. This surprising observation may stem from competing processes that accompany solvation, including a solvent-dependent reduction in the size of the Cotton effect and a solvent-specific displacement of the ORD curve. In analogy to the solvent-induced frequency shifts and intensity alterations that have been characterized extensively in conventional ultraviolet/visible absorption spectroscopy,<sup>42</sup> solvents are known<sup>15</sup> to shift the zero-crossing points of ORD traces and modify the overall amplitude of optical rotation, a phenomenon that becomes especially important for spectral regions containing strong electronic transitions. However, in the absence of detailed gas-phase measurements performed at several excitation wavelengths, this explanation remains, at best, speculative. A series of CDRP experiments designed to address this issue currently is underway in our laboratory.

Figure 4 contrasts ORD spectra obtained in cyclohexane solution with gas-phase measurements of specific rotation at 355 nm for (a) (*R*)-(+)-limonene, (b) (*S*)-(-)-propylene oxide, and (c) (1*S*,5*S*)-(-)- $\beta$ -pinene. As shown in this figure and reinforced by the numerical data compiled in Table 1, the solution-phase  $[\alpha]_{355\text{nm}}^{25^\circ\text{C}}$  values for limonene and  $\beta$ -pinene are respectively 37% higher and 69% lower than the corresponding isolated molecule quantities, reflecting, in part, the substantial role played by solvent-solute interactions. While the overall nuclear framework of  $\beta$ -pinene is expected to be fairly rigid, free rotation of the isopropenyl group in limonene can give rise to several low-lying energy minima in the ground electronic

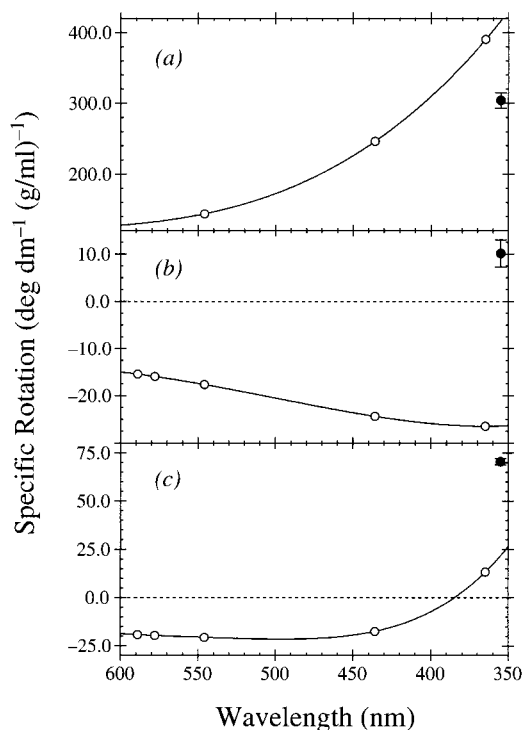


**Figure 4.** Gas-phase optical rotation of limonene, propylene oxide, and  $\beta$ -pinene compared with their solution-phase rotatory dispersion spectra. The specific optical rotations of (a) (*R*)-(+)-limonene, (b) (*S*)-(-)-propylene oxide, and (c) (1*S*,5*S*)-(-)- $\beta$ -pinene in units of  $\text{deg dm}^{-1} (\text{g/mL})^{-1}$  are plotted as a function of wavelength. In each panel, the open circular symbols connected by solid lines denote rotatory dispersion data obtained for cyclohexane solutions at the indicated discrete wavelengths. The CDRP-measured gas-phase rotation at 355 nm is signified by a filled circular symbol with the corresponding 1 standard deviation uncertainty limit given by the displayed error bars.

state, each of which has its own characteristic response to polarimetric measurements.<sup>43</sup> Consequently, solvent-induced modification of the isopropenyl torsional potential, leading to modification of conformational structures as well as a redistribution of their relative thermal populations, can strongly influence the observed optical activity. Ultimately, reliable *ab initio* predictions of the equilibrium geometries/energies and specific rotations exhibited by individual limonene conformers will be required to unravel the nature of such phenomena. Perhaps of even greater significance are the results obtained for propylene oxide, where, in addition to a dramatic change in the magnitude of  $[\alpha]_{355\text{nm}}^{25^\circ\text{C}}$ , the sign of the 355 nm optical rotation switches from negative to positive as one moves from a liquid cyclohexane medium to the rarefied vapor phase. This effect cannot be traced readily to near-resonant absorption processes (viz., the closest absorption features are reported<sup>44</sup> to reside below 180 nm) and is a subject of ongoing investigations; however, it does highlight the profound alterations in optical response that can be incurred through solvation. Indeed, a precedent exists in the case of propylene oxide for the occurrence of anomalously large solvent effects, with Kumata et al.,<sup>18</sup> reporting  $[\alpha]_{\text{D}}^{25^\circ\text{C}}$  parameters (viz., measured at the 589 nm sodium D line) for (*R*)-(+)-propylene oxide that range from  $+30.6^\circ \text{dm}^{-1} (\text{g/mL})^{-1}$  in benzene to  $-4.3^\circ \text{dm}^{-1} (\text{g/mL})^{-1}$  in water. Inversion of the ORD traces published by these authors (i.e., to account for the opposite behavior of optical enantiomers) suggests that the present gas-phase specific rotation at 355 nm for (*S*)-(-)-propylene oxide,  $+10.2 \pm 2.9^\circ \text{dm}^{-1} (\text{g/mL})^{-1}$ , most closely approximates the value found in an acetic acid medium.



Empirical methods for predicting the direction of the Cotton effect and, therefore, the sign of optical rotation in the vicinity of an absorption band have been formulated for a few special cases. In particular, the well-known octant rule,<sup>45</sup> based upon the classification of spatial arrangements exhibited by substituent groups, often succeeds when applied to the  $\pi^* \leftarrow n$  transitions of ketones (e.g., fenchone).<sup>46</sup> Similar ideas have been suggested for other chromophores,<sup>47</sup> including the  $\pi^* \leftarrow \pi$  systems of olefins; however, the fact that such  $\pi^* \leftarrow \pi$  resonances typically reside in the vacuum-ultraviolet region for unconjugated alkenes precludes straightforward analyses of near-ultraviolet and visible features, where ORD spectra also can exhibit extrema and zero-crossing points (cf. Figure 4) despite the apparent lack of accessible electronic manifolds. The sensitivity of optical behavior to structural alterations is demonstrated succinctly by Figures 3 and 4(c), which contain ORD data sets recorded respectively for the  $\alpha$ -pinene and  $\beta$ -pinene molecules. More specifically, as one moves toward shorter wavelengths, which correlates with a closer approach to characteristic  $\pi^* \leftarrow \pi$  resonances,  $\alpha$ -pinene shows the expected gradual increase in  $[\alpha]_{\lambda}^{25^\circ\text{C}}$  values, whereas the specific rotation of  $\beta$ -pinene is found to switch sign near 385 nm. Given the remote nature of the  $\pi^* \leftarrow \pi$  absorption in these unconjugated alkenes and the absence of other plausible electronically allowed transitions, this change in  $[\alpha]_{\lambda}^{25^\circ\text{C}}$  polarity is both surprising and, as of yet, unexplained. It is hoped that the present gas-phase work, by virtue of the glaring discrepancies it has uncovered with respect to traditional solution-phase results, will provide an impetus for future theoretical efforts designed to calculate ab initio the manifestation of optical activity in isolated molecular species and thereafter elucidate the mediation of optical response that accompanies solvation.

#### IV. Summary and Conclusions

Cavity ring-down polarimetry (CRDP), an ultrasensitive probe of circular birefringence and circular dichroism, has been developed and implemented for the interrogation of optical activity in chiral species maintained under rarefied gas-phase conditions. Built upon the burgeoning technique of cavity ring-down spectroscopy (CRDS),<sup>29</sup> as augmented by the incorporation of polarization elements into the resonator assembly, the light injection optics, and the signal detection train, this novel scheme has enabled the rotation rate of an interacting electromagnetic field to be followed over effective sample path lengths that readily exceed 1 km. Measurements of specific rotation values,  $[\alpha]_{\lambda}^T$  (in units of  $\text{deg dm}^{-1} (\text{g/mL})^{-1}$ ), were performed at ambient temperatures ( $T = 25^\circ\text{C}$ ) for  $\alpha$ -pinene,  $\beta$ -pinene, *cis*-pinane, limonene, fenchone, and propylene oxide, with the selected excitation wavelength of  $\lambda = 355$  nm being far removed from known electronic absorption features (i.e., with the possible exception of fenchone, where the  $\pi^* \leftarrow n$  transition peaks<sup>48</sup> at  $\sim 290$  nm). Direct comparison of these gas-phase results with analogous solution-phase data reveals the pronounced influence of complex solvent effects that can alter both the magnitude and the sign of the optical response, thereby highlighting the need for extending detailed investigations of isolated (gas-phase) molecules. Aside from elucidating the physical/optical ramifications of solvation processes, such gas-phase studies will furnish quantitative information that critically assesses ongoing theoretical calculations<sup>11,43</sup> designed to predict optical activity and absolute stereochemistry ab initio. While the present work has demonstrated the ability to resolve polarization rotation induced by (nonresonant) circular birefringence with an estimated sensitivity<sup>49</sup> to angle change of  $4 \times 10^{-8}$  rad  $\text{cm}^{-1}$  ( $2.5 \times$

$10^{-7}$ )°  $\text{cm}^{-1}$ ), the CRDP apparatus can be adapted easily for the observation of differential absorption signals stemming from (resonant) circular dichroism phenomena. Therefore, subject to the availability of suitable coatings for mirror and waveplate substrates, the CRDP methodology should enable high-resolution, gas-phase CD information to be acquired for resonant transitions residing in diverse spectral regions, including the fundamental (infrared) and overtone (near-infrared/visible) vibrational bands of chiral molecules.

By furnishing a unique probe of gas-phase circular birefringence/dichroism that combines high species sensitivity with quantitative analysis capabilities, the CRDP method could eventually find use in a variety of practical endeavors that demand the “chiral recognition” of volatile substances. For example, one might envision the engineering of such devices into modular optical activity detectors designed to monitor the effluent streaming from a gas chromatography (GC) column. However, the microgram-level detection limits demonstrated in the current study would be insufficient for reliable identification of the nanogram-scale materials emerging from typical analytical-grade GC instruments.<sup>50</sup> On the other hand, several steps can be taken to enhance the sensitivity of our CRDP apparatus. Aside from increasing the cavity dimensions and, therefore, the single-pass sample volume, the utilization of improved antireflection coatings on the intracavity waveplates should augment the effective interaction path length greatly, a fact highlighting the severe restriction on photon lifetimes incurred in the present resonator assembly by excessive losses from these internal components. Antireflection coatings having specified residual reflections as low as 0.01% per surface are available commercially and are being employed for the fabrication of a second-generation polarimeter. In addition, the exploitation of sophisticated polarization compensation schemes, in conjunction with superior mechanical and thermal stabilization of the ring-down cavity, should make the background-free detection of optical activity a viable option and eliminate the need to rely upon polarization modulation techniques (cf. section II). Finally, it is conceivable that innovations developed for enhancing sensitivity of the parent CRDS methodology (e.g., cavity mode control by means of “continuous wave” excitation<sup>32</sup> or “degenerate” cavity lengths)<sup>51</sup> could be implemented in a polarimetric configuration.

A variety of possible applications for the CRDP scheme follow from its ability to detect and analyze trace amounts of a chiral molecule in an environment composed primarily of achiral species. This trait would enable the gas-phase monitoring of volatile, optically active metabolites, including limonene and pinene, which have been examined during the present research effort. Consequently, information regarding biological systems (e.g., the growth and degradation of biomass)<sup>52</sup> could be obtained by means of a straightforward and nonintrusive optical measurement. For example, it has been suggested that the concentration of fungal metabolites in the vapor phase can serve as a quantitative indicator for the presence of mold growth in controlled environments.<sup>53</sup> In a similar manner, limonene, pinene, and other volatile monoterpenes have been the subject of numerous atmospheric and environmental studies, owing to their role in the formation of “natural” air pollution<sup>52,54</sup> (i.e., via biogenic hydrocarbons) as well as their potentially defensive capabilities against both insect<sup>55</sup> and mammalian<sup>56</sup> herbivores.

**Acknowledgment.** This work was performed under the auspices of grants provided by the National Science Foundation. P.H.V. gratefully acknowledges the Dreyfus Foundation for a Camille Dreyfus Teacher-Scholar Award and The Packard



Foundation for support through a Packard Fellowship for Science and Engineering. We wish to thank Dr. J. R. Cheeseman and Dr. M. J. Frisch (Gaussian, Inc.) for stimulating discussions.

## References and Notes

- Gaffield, W. *Stud. Nat. Prod. Chem.* **1990**, 7, 3. Crossley, R. *Tetrahedron* **1992**, 48, 8155. Eliel, E. L.; Wilen, S. H. *Stereochemistry of Organic Compounds*; Wiley: New York, 1994. Bentley, R. *Perspect. Biol. Med.* **1995**, 38, 188. Trigg, D. J. *Drug Discovery Today* **1997**, 2, 138. Bonner, W. A. *EXS* **1998**, 85, 159. Mislow, K. *Top. Stereochem.* **1999**, 22, 1.
- Stryer, L. *Biochemistry*; W. H. Freeman: New York, 1995.
- Snatzke, G. *Optical Rotatory Dispersion and Circular Dichroism in Organic Chemistry*; Heyden: London, 1967. Nakanishi, K.; Berova, N.; Woody, R. *Circular Dichroism: Principles and Applications*; VCH: New York, 1994. Fasman, G. D. *Circular Dichroism and the Conformational Analysis of Biomolecules*; Plenum Press: New York, 1996. Rodger, A.; Norden, B. *Circular Dichroism and Linear Dichroism*; Oxford University Press: Oxford, U.K., 1997.
- Le Bel, J. A. *Bull. Soc. Chim. Paris* **1874**, 22, 337.
- Cotton, A. C. R. *Hebd. Seances Acad. Sci.* **1895**, 120, 989.
- Biot, J.-B. *Mem. Acad. Sci.* **1817**, 2, 114.
- Gernez, D. *Ann. Sci. Ec. Norm. Sup.* **1864**, 1, 1. Guye, P.-A.; do Amaral, A.-P. *Arch. Sci. Phys. Nat.* **1895**, 33, 513.
- Bijvoet, J. M.; Peerdeman, A. F. *Nature* **1951**, 168, 271.
- Hehre, W. J.; Radon, L.; Schleyer, P. v. R.; Pople, J. A. *Ab Initio Molecular Orbital Theory*; Wiley: New York, 1986.
- Kondru, R. K.; Chen, C. H.-T.; Curran, D. P.; Beratan, D. N.; Wipf, P. *Tetrahedron* **1999**, 10, 4143. Kondru, R. K.; Wipf, P.; Beratan, D. N. *J. Phys. Chem. A* **1999**, 103, 6603.
- Cheeseman, J. R.; Frisch, M. J.; Devlin, F. J.; Stephens, P. J. *J. Phys. Chem. A* **2000**, 104, 1039.
- Lowry, T. M.; Gore, H. K. *Proc. R. Soc. London, Ser. A* **1932**, A135, 13.
- Aslanyan, V. M.; Minasyan, D. M. *Proceedings of Tepl. Dvizhenie Mol. Mezhmolekulyarnoe Vzaimodeistvie Zhidk. Rastvorakh, Mater. Mezhuuz. Nauch. Konf., 2nd, USSR, 1966*. Vuks, M. F., Ed.; Gos. Univ.: Samarkland, USSR, 1969.
- Mukhedkar, A. J. *J. Chem. Phys.* **1960**, 35, 2133. Coulombeau, C.; Rassat, A. *Bull. Soc. Chim. Fr.* **1966**, 12, 3752. Voisin, D.; Gastambide, B. *Bull. Soc. Chim. Fr.* **1971**, 7, 2643. Soczewinski, E.; Markowski, W. *Ann. Univ. Mariae Curie-Sklodowska, Sect. D* **1973**, 28, 9. Wozniak, S.; Linder, B. *Chem. Phys.* **1981**, 63, 377. Vul'fson, S. G.; Nikolaev, V. F. *Zh. Obshch. Khim.* **1983**, 53, 1153. Gottarelli, G.; Osipov, M. A.; Spada, G. P. *J. Phys. Chem.* **1991**, 95, 3879. Sanda, F.; Nakamura, M.; Endo, T. *Chem. Lett.* **1997**, 2, 175. Langeveld-Voss, B. M. W.; Christiaans, M. P. T.; Janssen, R. A. J.; Meijer, E. W. *Macromolecules* **1998**, 31, 6702.
- Reichardt, C. *Solvents and Solvent Effects in Organic Chemistry*; VCH: Weinheim, Germany, 1988.
- Bosnich, B. *J. Am. Chem. Soc.* **1967**, 89, 6143. Bosnich, B. In *Fundamental Aspects and Recent Developments in ORD and CD*; Ciardelly, F.; Salvadori, P., Eds.; Heyden: London, 1973; Chapter 3. Buckingham, A. D.; Stiles, P. J. *Acc. Chem. Res.* **1974**, 7, 258. Hayward, L. D. *Chem. Phys. Lett.* **1975**, 33, 53.
- Tokura, N.; Nagai, T.; Takenaka, S.; Oshima, T. *J. Chem. Soc., Perkin Trans. 2* **1974**, 337.
- Kumata, Y.; Furukawa, J.; Fueno, T. *Bull. Chem. Soc. Jpn.* **1970**, 43, 3920.
- Kronig, R. d. L. *J. Opt. Soc. Am.* **1926**, 12, 547. Kramers, H. A. *Atti. Congr. Int. Fis.* **1927**, 2, 545. Brachman, M. K. *Rev. Mod. Phys.* **1956**, 28, 393.
- Keiderling, T. A. *Appl. Spectrosc. Rev.* **1981**, 17, 189. Nafie, L. A. *Adv. Infrared Raman Spectrosc.* **1984**, 11, 49. Polavarapu, P. L. *Vib. Spectrosc. Struct.* **1984**, 13, 103. Stephens, P. J.; Lowe, M. A. *Annu. Rev. Phys. Chem.* **1985**, 36, 213. Keiderling, T. A. *Nature* **1986**, 322, 851. Freedman, T. B.; Nafie, L. A. *Top. Stereochem.* **1987**, 17, 113.
- Nafie, L. A. *Annu. Rev. Phys. Chem.* **1997**, 48, 357.
- Barron, L. D. *Acc. Chem. Res.* **1980**, 13, 90. Barron, L. D. *Vib. Spectrosc. Struct.* **1989**, 17B, 343. Barron, L. D.; Hecht, L. *Biomolecular Spectroscopy*; Wiley: Chichester, U.K., 1993; Part B, Vol. 21. Barron, L. D.; Hecht, L.; Bell, A. F. *Appl. Spectrosc.* **1996**, 50, 619.
- Polavarapu, P. L.; Michalska, D. F. *J. Am. Chem. Soc.* **1983**, 105, 6190. Cianciosi, S. J.; Spencer, K. M.; Freedman, T. B.; Nafie, L. A.; Baldwin, J. E. *J. Am. Chem. Soc.* **1989**, 111, 1913. Freedman, T. B.; Spencer, K. M.; McCarthy, C.; Cianciosi, S. J.; Baldwin, J. E.; Nafie, L. A.; Moore, J. A.; Schwab, J. M. *Proc. SPIE Int. Soc. Opt. Eng.* **1989**, 1145, 273. Freedman, T. B.; Spencer, K. M.; Ragunathan, N.; Nafie, L. A. *Can. J. Chem.* **1991**, 69, 1619.
- Kawiecki, R. W.; Devlin, F. J.; Stephens, P. J.; Amos, R. D. *J. Phys. Chem.* **1991**, 95, 9817.
- Aamouche, A.; Devlin, F. J.; Stephens, P. J. *Chem. Commun. (Cambridge)* **1999**, 4, 361. Deng, Z.; Polavarapu, P. L.; Ford, S. J.; Hecht, L.; Barron, L. D.; Ewing, C. S.; Jalkanen, K. *J. Phys. Chem.* **1996**, 100, 2025. Stephens, P. J.; Ashvar, C. S.; Devlin, F. J.; Cheeseman, J. R.; Frisch, M. J. *Mol. Phys.* **1996**, 89, 579. Barron, L. D.; Hecht, L.; Wilson, G. *Biochemistry* **1997**, 36, 13143. Chabalowski, C. F.; Jenson, J. O.; Stephens, P. J.; Devlin, F. J.; Stephens, P. J.; Cheeseman, J. R.; Frisch, M. J. *J. Phys. Chem. A* **1997**, 101, 9912. Devlin, F. J.; Stevens, P. J.; Cheeseman, J. R.; Frisch, M. J. *J. Phys. Chem. A* **1997**, 101, 6322. Han, W.-G.; Jalkanen, K. J.; Elstner, M.; Suhai, S. *J. Phys. Chem. B* **1998**, 102, 2587.
- Mason, M. G.; Schnepf, O. *J. Chem. Phys.* **1973**, 59, 1092.
- Schnepf, O.; Allen, S.; Pearson, E. F. *Rev. Sci. Instrum.* **1970**, 41, 1136. Johnson, W. C. *Rev. Sci. Instrum.* **1971**, 42, 1283. Gross, K. P.; Schnepf, O. *Chem. Phys. Lett.* **1975**, 36, 531. Levi, M.; Cohen, D.; Schurig, V.; Basch, H.; Gedanken, A. *J. Am. Chem. Soc.* **1980**, 102, 6972.
- Poirson, J.; Vallet, M.; Bretenaker, F.; Le Floch, A.; Thépot, J.-Y. *Anal. Chem.* **1998**, 70, 4636.
- Romanini, D.; Lehmann, K. K. *J. Chem. Phys.* **1993**, 99, 6287. Zalicki, P.; Zare, R. N. *J. Chem. Phys.* **1995**, 102, 2708. Hodges, J. T.; Looney, J. P.; van Zee, R. D. *J. Chem. Phys.* **1996**, 105, 10278. Hodges, J. T.; Looney, J. P.; van Zee, R. D. *Appl. Opt.* **1996**, 35, 4112. Scherer, J. J.; Paul, J. B.; O'Keefe, A.; Saykally, R. J. *Chem. Rev.* **1997**, 97, 25. Wheeler, M. D.; Newman, S. M.; Orr-Ewing, A. J.; Ashfold, M. N. R. *J. Chem. Soc., Faraday Trans.* **1998**, 94, 337.
- Anderson, D. Z.; Frisch, J. C.; Masser, C. S. *Appl. Opt.* **1984**, 23, 1238.
- O'Keefe, A.; Deacon, D. A. G. *Rev. Sci. Instrum.* **1988**, 59, 2544.
- Meijer, G.; Boogarts, M. G. H.; Jongma, R. T.; Parker, D. H. *Chem. Phys. Lett.* **1994**, 217, 112. Engeln, R.; Meijer, G. *Rev. Sci. Instrum.* **1996**, 67, 2708. Engeln, R.; von Helden, G.; Berden, G.; Meijer, G. *Chem. Phys. Lett.* **1996**, 262, 105. Martin, J.; Paldus, B. A.; Zalicki, P.; Wahl, E. H.; Owano, T. G.; Harris, J. S., Jr.; Kruger, C. H.; Zare, R. N. *Chem. Phys. Lett.* **1996**, 258, 63. Romanini, D.; Kachanov, A. A.; Sadeghi, N.; Stoeckel, F. *Chem. Phys. Lett.* **1997**, 264, 316. Levenson, M. D.; Paldus, B. A.; Spence, T. G.; Harb, C. C.; Harris, J. S., Jr.; Zare, R. N. *Chem. Phys. Lett.* **1998**, 290, 335.
- Romanini, D.; Kachanov, A. A.; Sadeghi, N.; Stoeckel, F. *Chem. Phys. Lett.* **1997**, 264, 316.
- Engeln, R.; Berden, G.; van den Berg, E.; Meijer, G. *J. Chem. Phys.* **1997**, 107, 4458.
- Sakurai, J. J. *Modern Quantum Mechanics*; Addison-Wesley: Reading, MA, 1994.
- Barron, L. D. In *New Developments in Molecular Chirality*; Mezey, P. G., Ed.; Kluwer Academic: Dordrecht, The Netherlands, 1991; Vol. 5, p 293.
- Xu, Z.; Zhang, J.; Jiang, Y.; Huang, H. *Jil. Dax. Zir. Kex. Xuebao* **1991**, 1, 73. Tereshko, A. B.; Basalaeva, L. I.; Kozlov, N. G.; Tarasevich, V. A. *Zh. Org. Khim.* **1996**, 32, 823.
- Müller, T.; Wiberg, K. B.; Vaccaro, P. H. Manuscript in preparation.
- Müller, T.; Vaccaro, P. H. *Chem. Phys. Lett.* **1997**, 266, 575. Müller, T.; Vaccaro, P. H. *Rev. Sci. Instrum.* **1998**, 69, 406. Müller, T.; Vaccaro, P. H.; Pérez-Bernal, F.; Iachello, F. *J. Chem. Phys.* **1999**, 111, 5038.
- Jones, R. J. *J. Opt. Soc. Am.* **1941**, 31, 488. Jones, R. C. *J. Opt. Soc. Am.* **1941**, 31, 493. Hurwitz, H., Jr.; Jones, R. C. *J. Opt. Soc. Am.* **1941**, 31, 500. Jones, R. C. *J. Opt. Soc. Am.* **1942**, 32, 486.
- Onsager, L. *J. Am. Chem. Soc.* **1936**, 58, 1486.
- Aagren, H.; Mikkelsen, K. V. *THEOCHEM* **1991**, 80, 425. Kawski, A. *Photochem. Photophys.* **1992**, 5, 1. Reichardt, C. *Chem. Rev.* **1994**, 94, 2319.
- Cheeseman, J. R. Personal communication.
- Cohen, D.; Levi, M.; Basch, H.; Gedanken, A. *J. Am. Chem. Soc.* **1983**, 105, 1738. Carnell, M.; Peyerimhoff, S. D.; Breest, A.; Gödderz, K. H.; Ochmann, P.; Hormes, J. *Chem. Phys. Lett.* **1991**, 180, 477.
- Djerassi, J. *Optical Rotatory Dispersion and Its Applications to Organic Chemistry*; McGraw-Hill: New York, 1960. Moffitt, W.; Woodward, R. B.; Moscovitz, A.; Klyne, W.; Djerassi, C. *J. Am. Chem. Soc.* **1961**, 83, 4013.
- Korvola, J.; Malkonen, P. *J. Suom. Kemistil. B* **1972**, 45, 381.
- LeGrand, M.; Rougier, M. J. *Application of Optical Activity to Stereochemical Determinations: Fundamentals and Methods*; Georg Thieme Verlag: Stuttgart, Germany, 1977; Vol. 2. Charney, E. *The Molecular Basis of Optical Activity: Optical Rotatory Dispersion and Circular Dichroism*; Wiley: New York, 1979. Snatzke, G. *Angew. Chem., Int. Ed. Engl.* **1979**, 18, 363.
- Pulm, F.; Schramm, J.; Hormes, J.; Grimme, S.; Peyerimhoff, S. D. *Chem. Phys.* **1997**, 224, 143.
- This CDRP sensitivity is comparable to the  $10^{-8}$  rad/cm value reported for the measurement of magnetically induced polarization effects by Engeln, et al. in reference [34] and is substantially better than the  $\leq 0.002^\circ \text{ dm}^{-1}$  ( $\leq 3.5 \times 10^{-6}$  rad  $\text{cm}^{-1}$ ) sensitivity specified for the commercial polarimeter employed in the present solution-phase studies.

(50) Baugh, P. J. *Gas Chromatography: A Practical Approach*; Oxford University Press: Oxford, U.K., 1993. McNair, H. M.; Miller, J. M. *Basic Gas Chromatography*; Wiley: New York, 1998.

(51) Kachanov, A. A.; Panov, S. I.; Dubinski, I.; Ruslen, L. M.; Silva, M. L.; Field, R. W. *Proceedings of 53rd International Symposium on Molecular Spectroscopy*, Columbus, OH, 1998. Sessions MI09 and MI10.

(52) Fuentes, J. D.; Wang, D.; Neumann, H. H.; Gillespie, T. J.; Den Hartog, G.; Dann, T. F. *J. Atmos. Chem.* **1996**, 25, 67.

(53) Bock, R.; Schleichinger, H.; Ruden, H. *Umweltmed. Forsch. Prax.* **1998**, 3, 359.

(54) Corchnoy, S. B.; Arey, J.; Atkinson, R. *Atmos. Environ. Part B* **1992**, 26, 339. Seinfeld, J. H.; Pandis, S. N. *Atmospheric Chemistry and Physics: From Air Pollution to Climate Change*; Wiley: New York, 1998.

(55) Cates, R. G.; Redak, R. A. *Natural Resistance of Plants to Pests: Roles of Allelochemicals*; ACS Symp. Ser. 296; American Chemical Society: Washington, DC, 1986; p 106. Ross, D. W.; Birgersson, G.; Espelie, K. E.; Berisford, C. W. *Can. J. Bot.* **1995**, 73, 21.

(56) Duncan, A. J.; Hartley, S. E.; Iason, G. R. *Can. J. Zool.* **1994**, 72, 1715.